Controlled Precipitation of Zinc Oxide Particles at Room Temperature

Ana Paula A. Oliveira,*,† Jean-François Hochepied,† François Grillon,‡ and Marie-Hélène Berger‡

Centre d'Energétique, Laboratoire Systèmes Colloïdaux dans les Procédés Industriels, Ecole des Mines de Paris, 60 Boulevard Saint-Michel 75006 Paris Cedex 06, and Centre des Matériaux, Ecole des Mines de Paris, BP 87 91003 Evry Cedex, France

Received December 6, 2002. Revised Manuscript Received March 31, 2003

Zinc nitrate precipitated with NaOH solution at room temperature under double-jet conditions produced micrometric zinc oxide particles with ellipsoid or starlike morphology separated by only a slight variation of pH (9.5 and 10.5, respectively). The formation kinetics of starlike particles was followed by SEM observations, suggesting that they result from a solid-state transformation of the hydroxide matrix. This mechanism involved the nucleation of 30-nm ZnO particles inside the matrix, followed by their aggregation into starlike particles. The introduction of sodium sulfate or sodium dodecyl sulfate in the bath before precipitation led to a drastic size reduction and to a diversity of particle shapes (from half-ellipsoids to full ellipsoids). The presence of these additives provided important hints on particle formation and confirmed that submicronic particles resulted from nanocrystals oriented aggregation.

Introduction

Several studies on the synthesis of zinc oxide (ZnO) particles have been performed in recent decades because of the diversified industrial applications of this material. Among these applications, major interests concern catalytic,[1,2] luminescent,[3,4] and electronic (e.g., varistors, semiconductors, and gas sensors) devices,[5−7] pigments,[8] and components for the pharmaceutical and cosmetic industries.[9,10]

In the literature, chemical routes[11−18] are presented as the most commonly used methods for synthesizing ZnO, while evaporation techniques[19,20] are restricted to the production of whisker- or tetrapod-shaped ZnO particles. Precipitation processes make possible the production of large quantities of ceramic oxides in a reproducible way. Nevertheless, intermediate compounds, depending on the zinc precursor salt, are usually precipitated and then transformed into zinc oxide by thermal decomposition processes. Some authors[13,14] handled this constraint by using hydrothermal processes to precipitate ZnO at lower temperatures (100−220 °C). Alternatively, Zhong and Matijevic[18] used a controlled double-jet precipitation process to prepare uniform ZnO particles without a further thermal decomposition process. However, the precipitation temperature was fixed at 90 °C, which can still be considered a high temperature for this process.

A wide variety of ZnO particle shapes was observed depending on synthesis conditions, but despite the number of precipitation procedures, some points still require clarification, such as the mechanisms that define the final particle shape. Two important mechanism descriptions are usually considered: (a) (mono)-crystal growth habit and dissolution/recrystallization phenomena[21] or (b) nanoparticles oriented aggregation.[18]

The goals of this work were, initially, to directly precipitate ZnO particles at room temperature in a nonpressurized system, and, subsequently, to evaluate

* Corresponding author. Fax: +33 1 43 26 59 10. E-mail: oliveira@paris.ensmp.fr.
† Centre d'Energétique.
‡ Centre des Matériaux.

(1) Gouvêa, C. A. K.; Wypych, F.; Moraes, S. G.; Durán, N.; Nagata, N.; Peralta-Zamora, P. *Chemosphere* **2000**, *40*, 433.
(2) Elseviers, W.; Verelst, H. *Fuel* **1999**, *78*, 601.
(3) Fujihara, S.; Naito, H.; Kimura, T. *Thin Solid Films* **2001**, *389*, 227.
(4) Lorenz, C.; Emmerling, A.; Fricke, J.; Schmidt, T.; Hilgendorff, M.; Spanhel, L.; Müller, G. *J. Non-Cryst. Solids* **1998**, *238*, 1.
(5) Degen, A.; Kosec, M. *J. Eur. Ceram. Soc.* **2000**, *20*, 667.
(6) Look, D. C.; Reynolds, D. C.; Sizelove, J. R.; Jones, R. L.; Litton, C. W.; Cantwell, G.; Harsch, W. C. *Solid State Commun.* **1998**, *105* (6), 399.
(7) Wrzesinski, J.; Fröhlich, D. *Solid State Commun.* **1998**, *105* (5), 301.
(8) Sigoli, F. A.; Davolos, M. R.; Jafelicci, M., Jr. *J. Alloys Compd.* **1997**, *262−263*, 292.
(9) Yamamoto, O. *Int. J. Inorg. Mater.* **2001**, *3*, 643.
(10) Akiyama, H.; Yamasaki, O.; Kanzaki, H.; Tada, J.; Arata, J. *J. Dermatol. Sci.* **1998**, *17*, 67.
(11) Rodriguez-Paez, J. E.; Caballero, A. C.; Villegas, M.; Moure, C.; Durán, P.; Fernández, J. F. *J. Eur. Ceram. Soc.* **2001**, *21*, 925.
(12) Komarnemi, S.; Bruno, M.; Mariani, E. *Mater. Res. Bull.* **2000**, *35*, 1843.
(13) Lu, C.-H.; Yeh, C.-H. *Ceram. Int.* **2000**, *26*, 351.
(14) Chen, D. O.; Jiao, X.; Cheng, G. *Solid State Commun.* **2000**, *113*, 363−366.
(15) Reverchon, E.; Della Porta, G.; Sannino, D.; Ciambelli, P. *Powder Technol.* **1999**, *102*, 127.
(16) Lu, C.-H.; Yen, C.-H. *Mater. Lett.* **1997**, *33*, 129.
(17) Lim, B. P.; Wang, J.; Ng, S. C.; Chew, C. H.; Gan, L. M. *Ceram. Int.* **1998**, *24*, 205.
(18) Zhong, Q.; Matijevic, E. *J. Mater. Chem.* **1996**, *6* (*3*), 443.
(19) Hu, J. Q.; Ma, X. L.; Xie, Z. Y.; Wong, N. B.; Lee, C. S.; Lee, S. T. *Chem. Phys. Lett.* **2001**, *34*, 97.
(20) Wu, R.; Xie, C.; Xia, H.; Hu, J.; Wang, A. *J. Crystal Growth* **2000**, *217*, 274.
(21) Öner, M.; Norwig, J.; Meyer, W. H.; Wegner, G. *Chem. Mater.* **1998**, *10*, 460.

10.1021/cm0213725 CCC: $25.00
Published on Web 07/18/2003

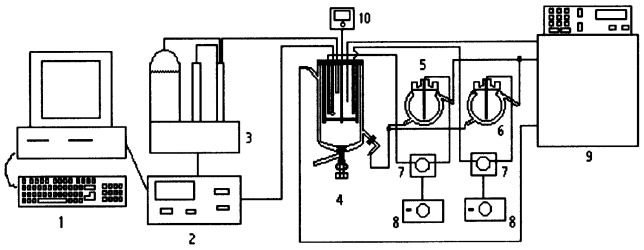

Figure 1. Schematic representation of precipitation apparatus: 1, computer; 2, pH meter; 3, automatic buret; 4, reactor; 5, zinc salt reservoir; 6, NaOH reservoir; 7, peristaltic pump; 8, peristaltic pump velocity controller; 9, thermostatic bath; 10, mechanical agitator.

the mechanism involved in the formation of ZnO submicrometric particles.

Experimental Section

Precipitation Procedures. Zinc nitrate ($Zn(NO_3)_2 \cdot 6H_2O$) and zinc sulfate ($ZnSO_4 \cdot 7H_2O$), both 99% purity, were adopted as the source material for zinc species. Sodium hydroxide (NaOH, flakes, 97% purity) was employed as the base for all experiments. Sodium sulfate (SS, $Na_2SO_4 \cdot 10H_2O$) and sodium dodecyl sulfate (SDS, $H_3(CH_2)_{11}OSO_3Na$) (99% and 98% purity, respectively), were chosen as the additives to be evaluated. All reagents were purchased from Prolabo.

Two solutions were prepared as follows: solution A − 0.1 mol $Zn(NO_3)_2$ or $ZnSO_4$ dissolved in 0.2 dm^3 distilled water; and solution B − 0.2 mol NaOH in 0.2 dm^3 distilled water.

Solutions A and B were injected into a standard double-walled, water-jacketed, thermostated (25 or 60 °C) hemispheric reactor (V = 1.5 dm^{-3}) by double jet at a flow rate of 2.8 × 10^{-4} $dm^3 \cdot min^{-1}$ controlled by peristaltic pumps. The reactor was filled with 0.6 dm^3 of distilled water or with a solution containing 0.2 mol SS or 0.2 mol SDS, depending on the experiment. The inside of the reactor was composed of four Teflon baffles to reduce the vortex into the vessel, a propeller with four 45°-tilted blades stirring at 500 rpm, a pH combined electrode, and a temperature probe. The pH was adjusted with a 1 mol·dm^{-3} NaOH solution, and the temperature was recorded by a pH-controller radiometer PHM290 coupled with a computer.

After the addition of reagents, the mixture was stirred for 2 h at regulated pH and temperature. The precipitate was washed with distilled water, frozen, and subsequently vacuum-dried. Figure 1 is a schematic presentation of the precipitation apparatus.

Characterization Techniques. Dried-powder X-ray patterns were recorded on a Bruker D8 diffractometer in $\theta-\theta$ configuration, with cobalt Kα radiation (λ = 1,789 Å), and equipped with a position-sensitive detector. The X-ray powder diffraction (XRD) was used to identify the precipitated powder crystalline phases and to estimate crystallite size using the Scherrer formula

$$L(hkl) = \frac{0.9\lambda}{\Delta(hkl)\cos\theta} \quad (1)$$

where λ is the X-ray wavelength, θ the Bragg's angle, and Δ is the full width of the diffraction line (hkl) at half of maximum intensity.

Scanning (SEM-Zeiss Leo 982) and transmission (TEM-Philips EM430, operating at 300 kV) electron microscopies were used to investigate particle morphology and size.

Results and Discussion

Precipitation with Zinc Nitrate and Sodium Hydroxide. *In Distilled Water*. Table 1 presents a summary of experimental conditions and the results of the precipitation tests with zinc nitrate and sodium hydroxide in distilled water.

DRX analysis for tests 1−4 showed that ZnO was precipitated directly from the solution, and, consequently, no further thermal decomposition step was necessary. Figure 2 depicts a typical spectrum obtained in our experiments. It was in accordance with JCPDS index[22] related to zincite, ZnO ($P63mc$, cell parameters: $a = b$ = 3.250 Å and c = 5.207 Å). In the range limited by our experimental conditions, pH and temperature variations did not affect the crystalline structure of the precipitated phase.

At room temperature, the direct synthesis of zinc oxide rather than the more or less well-crystallized zinc hydroxide is not necessarily expected: published thermodynamic data have not led to any definite conclusion, and in fact put forth recurrent questioning.[23] Besides, precipitation generally involves several transformations from an amorphous hydroxide, to a crystallized hydroxide, then to the oxide. In many metallic ions systems there is no doubt about the expected final product nature, either crystallized hydroxide or the oxide, but with zinc salt at low temperature we deal with a borderline case. Generally, precipitation procedures use high temperatures to force hydrolysis leading to zinc oxide, but for a better understanding of the oxide phase formation it was found more instructive to choose the softest possible conditions that allow the direct precipitation of zinc oxide particles.

The crystallite size was estimated for (100), (002), and (101) diffraction lines. For all experiments, the crystallite sizes calculated for (100) and (101) were almost the same, however for (002) a 50% higher value was generally obtained. This result indicated a preferential growth along the *c*-axis leading to slightly elongated crystallites (Table 1).

The precipitation at 25 °C and pH 9.5 produced ellipsoidal particles with dimensions around 500 nm × 1100 nm (Figure 3). From TEM and SEM observations, as well as from crystallite size measurements, these particles consisted of an assembly of 30−40 nm diameter nanocrystals. This mechanism was in accordance with the observations of Zhong and Matijevic[18] and with the model developed by Park et al.[24] for the formation of monodispersed colloids. They considered a two-stage growth process: nucleation/growth of primary particles, and formation of secondary particles by primary particles aggregation.

It is suggested that particle aggregation followed a preferential orientation of crystallites, probably as a result of polar behavior of crystals in relation to the *c*-axis. The polarity of ZnO crystals has been studied by Li et al.,[25] Wander and Harrison,[26] and Wander et al.[27] The importance of dipolar effects in particles alignment and further growth has been evidenced for

(22) Joint Committee on Powder Diffraction Standards. *Powder Diffraction File*, card no. 36-1451.
(23) Zhang, Y.; Muhammed, M. *Hydrometallurgy* **2001**, *60*, 215.
(24) Park, J.; Privman, V.; Matijevic, E. *J. Phys. Chem. B* **2001**, *105*, 11630.
(25) Li, W.-J.; Shi, E.-W.; Zhong, W.-Z.; Yin, Z.-W. *J. Crystal Growth* **1999**, *203*, 186.
(26) Wander, A.; Harrison, N. M. *Surf. Sci. Lett.* **2000**, *457*, L342.
(27) Wander, A.; Schedin, F.; Steadman, P.; Norris, A.; McGrawth, R.; Turner, T. S.; Thornton, G.; Harrison, N. M. *Phys. Rev. Lett.* **2001**, *86* (17), 3811.

Table 1. Summary of Experimental Conditions and Results of the Precipitation Tests with Zinc Nitrate and Sodium Hydroxide in Distilled Water

test no.	pH	*T* (°C)	particle morphology and size	crystal size (nm)
1	9.5	25	ellipsoidal 500 × 1000 nm	17 × 28
2	10.5	25	starlike 1000 nm	16 × 27
3	9.5	60	ellipsoidal 150−1000 nm	22 × 31
4	10.5	60	ellipsoidal and spherical 100−1000 nm	23 × 31

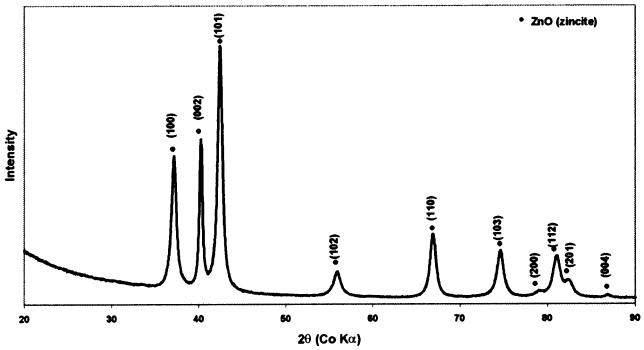

Figure 2. Typical X-ray diffraction pattern of ZnO powder prepared by double-jet precipitation with $Zn(NO_3)_2$ and NaOH for different experimental conditions.

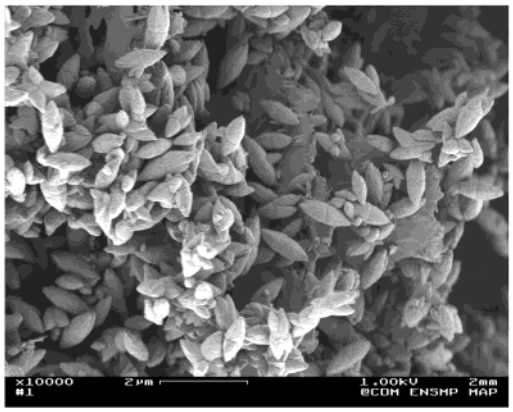

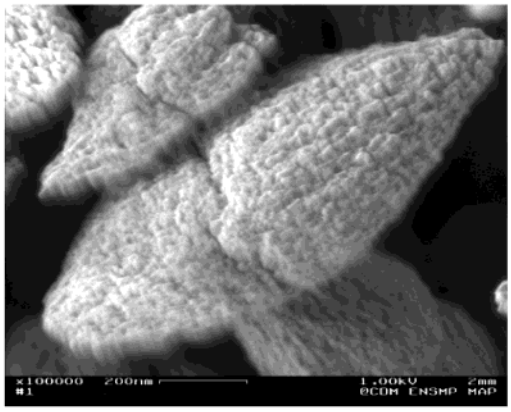

Figure 3. SEM micrographs of ellipsoidal ZnO particles precipitated from zinc nitrate with sodium hydroxide at pH 9.5, 25 °C.

other materials.[27,28] Isotropic structures made up of aggregated ZnO nanocrystallites were also observed by Rodriguez-Paez et al.[11] However, in this last case, agglomerates were obtained by a rather indirect process with washing and thermal treatment as important stages to obtain the final product. An unusual feature of our samples was the occurrence of a crack, perpendicular to the length, in the middle of the particle, and sometimes also along the length, with rare occurrences of a well-separated splitting.

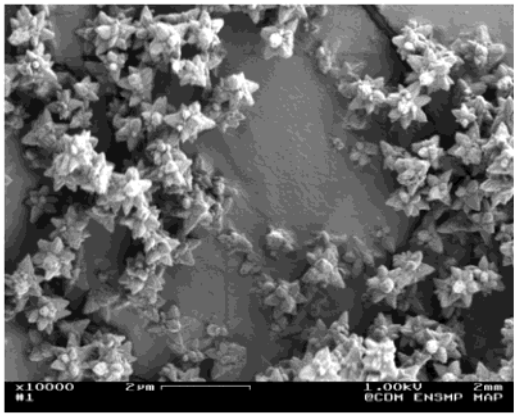

Figure 4. SEM micrograph of starlike ZnO particles obtained by precipitation of zinc nitrate with sodium hydroxide at pH 10.5, 25 °C.

Starlike particles (1 μm), also called intertwinned ellipsoids or intertwinned needles depending on the lengths of the branches, were formed at 25 °C and pH 10.5 as shown in Figure 4. This morphology was also obtained by Li and Haneda[29] for a system consisting of 0.01 mol·dm^{-3} $Zn(NO_3)_2$ and 0.02 mol·dm^{-3} hexamethylenetetraamine at 90 °C. Despite using a low salt concentration, the authors obtained approximately 3-μm particles. Using NaOH instead of an amine base, Komarneni et al.[12] produced a more heterogeneous sample that included some 2-μm starlike particles, by the precipitation of 0.1 mol·dm^{-3} $Zn(NO_3)_2$ at pH 12, T = 50 °C, during 15 min by using microwaves. In this last case, the authors attributed the precipitation of such a particular shape to the use of microwaves, but our present results evidence that other parameters are responsible for the formation of a star-type morphology.

To understand better the formation of starlike particles, a kinetics study was performed. As exhibited in Figure 5, the initially precipitated $Zn(OH)_2$ matrix underwent significant transformation until $t = 60$ min. Initially ($t = 5$ min), the hydroxide matrix seemed to be formed by particles of indeterminate shape and size, then was subsequently transformed into thin sheets ($t = 15$ min). At $t = 30$ min, the $Zn(OH)_2$ matrix was a combination of sheets and an unshaped structure (Figure 5(c)). At $t = 45$ min, intermediate states were composed by a mixture of $Zn(OH)_2$ matrix and starlike particles with their final aspect and dimensions. After 90 min the sample was mainly composed of ZnO particles. In resume, the kinetics study exhibited a sudden sprouting of well-shaped stars from an ill-shaped $Zn(OH)_2$ matrix with only a few identified intermediates. Some observations suggested that ZnO particles appeared directly in the $Zn(OH)_2$ matrix rather than on the surface of the $Zn(OH)_2$ sheets.

(28) Tang, Z.; Kotov, N.; Giersig, M. *Science* **2002**, *297*, 237.
(29) Li, D.; Haneda, H. *Chemosphere* **2003**, *51*, 129.

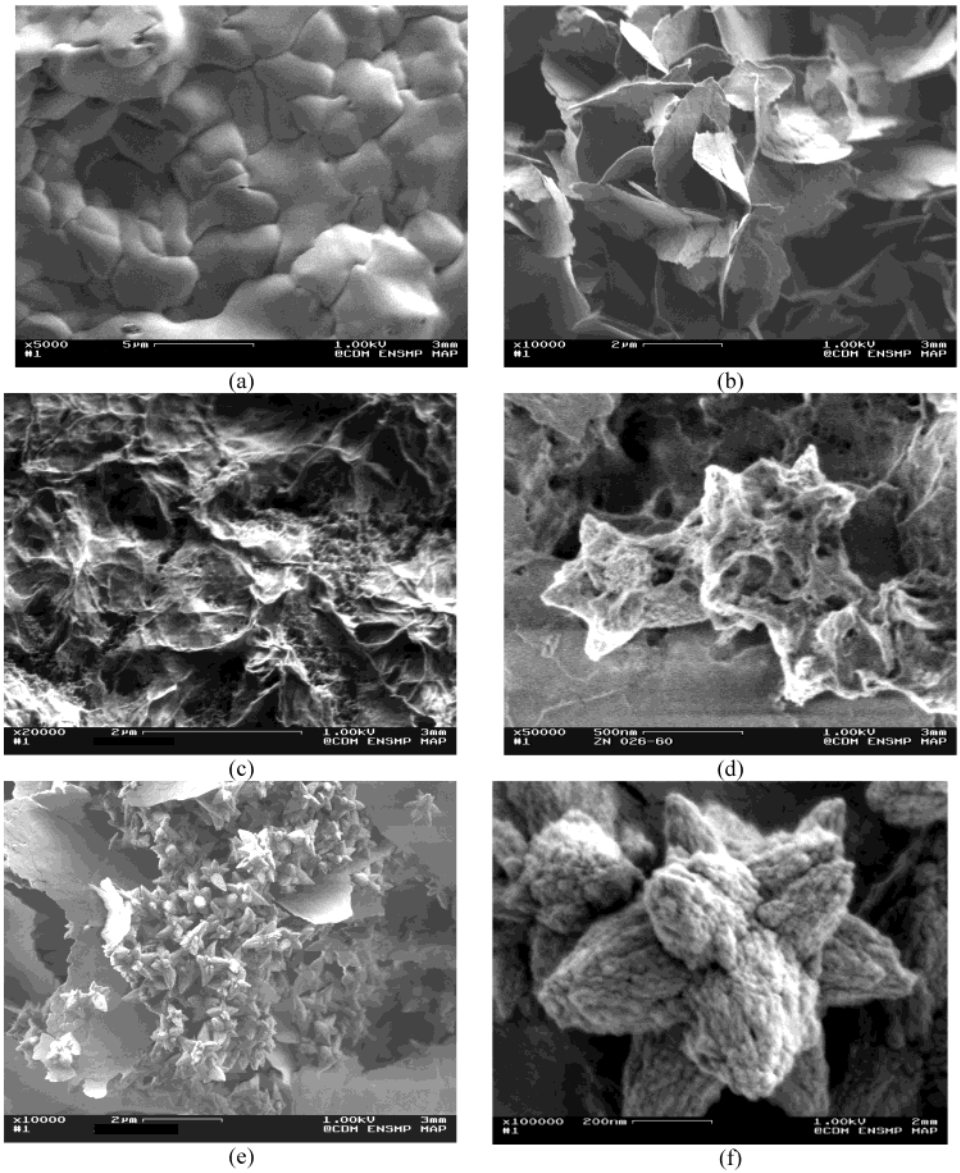

Figure 5. Kinetics study: SEM micrographs of ZnO particles obtained at pH 10.5, 25 °C by precipitation of zinc nitrate with sodium hydroxide at (a) $t = 5$ min; (b) $t = 15$ min (c) $t = 30$ min; (d) $t = 60$ min; (e) $t = 90$ min; and (f) $t = 120$ min.

At a higher temperature of 60 °C, at pH 9.5, ellipsoids with a particle size from 150 nm to 1 μm were precipitated (Figure 6). A similar morphology was obtained for pH 10.5, however, spherical particles were occasionally observed. This sample was clearly less homogeneous than that at lower temperature, with particle size varying from 100 nm to 1 μm. The occurrence of isolated small particles for both pH values indicated that a temperature rise might lead to limitation of nanoparticle aggregation into a more complex morphology such as starlike.

Additives Effect on the Formation of Zinc Oxide Particles. As seen previously, a direct kinetics study did not exhibit embryos of final zinc oxide particles, so additives were used to block their formation. Table 2 shows the experimental conditions of the precipitation tests with zinc nitrate and sodium hydroxide in the presence of additives (sodium sulfate and sodium dodecyl sulfate) and the main results.

X-ray diffraction patterns obtained for tests 5−8 showed that the precipitated product was pure ZnO

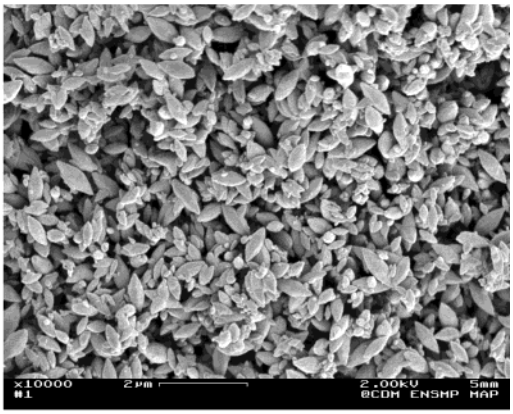

Figure 6. SEM micrographs of ZnO particles precipitated from zinc nitrate with sodium hydroxide at pH 9.5, 60 °C.

(JCPDS index[22] for zincite). In the presence of additives (SS or SDS) for zinc nitrate system, the difference between crystallite sizes calculated for (100)/(101) and (002) diffraction lines was also evident. They varied from

Table 2. Summary of Experimental Conditions and Results of the Precipitation Tests with Zinc Nitrate and Sodium Hydroxide in the Presence of Additives

test no.	pH	*T* (°C)	additive	particle morphology and size	crystal size (nm)
5	10.5	25	SS	half-ellipsoidal 450 nm	19 × 26
6	10.5	25	SDS	half-ellipsoidal 200 nm asymmetrical ellipsoidal ellipsoidal 350 nm small particles 30 nm	17 × 26
7	10.5	60	SS	half-ellipsoidal 250 nm small particles 30 nm	20 × 32
8	10.5	60	SDS	half-ellipsoidal 140 nm	21 × 31

14 to 18 nm for the first two reflections, to 26 nm for the latter at 25 °C. No significant influence of the additives on the crystallite size was observed.

Sodium sulfate (SS) is well-known to hamper oxides or hydroxides crystal growth. The purpose of investigating zinc oxide precipitation from zinc nitrate solution in sulfate medium at pH 10.5 was to evaluate its capacity for hindering the assembly of nanocrystals into particles. Pure ZnO phase was precipitated with the same crystallite dimensions as measured for particles precipitated in distilled water. This could confirm nucleation and growth of oxide nanocrystallites had occurred in the bulk of solid zinc hydroxide, relatively protected from environment. The presence of SS led to a substantial modification of particle shape and size (Figure 7a): mainly half-ellipsoids (200 nm × 450 nm) were obtained. In this case, instead of obstructing crystal growth, sodium sulfate limited the aggregation of nanocrystallites. Half-ellipsoids might represent the separate branches of starlike particles and confirmed the strong oriented aggregation tendency of zinc oxide nanocrystals.

Sodium dodecyl sulfate (SDS) was also evaluated as an additive. SDS forms direct micelles in the bath, therefore the charged interface may have an influence on precursor nucleation (favorable sites), on phase transformations (by modification of hydroxide surfaces) and on final agglomeration in bigger particles (if surfactant molecules stick to some faces of crystallites).

Figure 7b shows that, in the presence of SDS at 25 °C and pH 10.5, ZnO particles presented various morphologies, such as half-ellipsoids (150−200 nm long), asymmetrical ellipsoids composed of different-sized half-ellipsoids, and, finally, symmetrical ellipsoids (115 nm × 350 nm). Among these almost complete ellipsoids many 30-nm-diameter particles were observed; they were probably individual building blocks of observed structures. From SS and SDS results, the formation of ellipsoids might result from the aggregation of nanoparticles into half ellipsoids, followed by germination and growth of a second half at the bases. The formation of starlike particles might follow the same principle, considering also perpendicular germination.

At 60 °C, we observed a size reduction of (ill-shaped) half-ellipsoid particles precipitated in SS solution (100 nm × 250 nm) and the occurrence of 30-nm particles. At the same temperature, in the presence of SDS, only half-ellipsoids smaller than 60 nm × 140 nm were obtained.

Zhong and Matijevic[18] also observed the expressive reduction in particle size when SDS was added in the reactor. However, for their system, the presence of this surfactant also significantly decreased crystallite size.

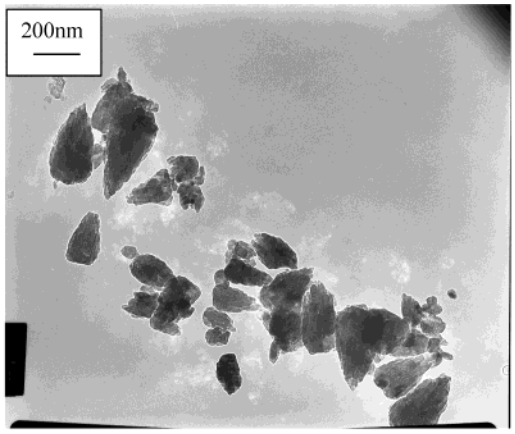

(a)

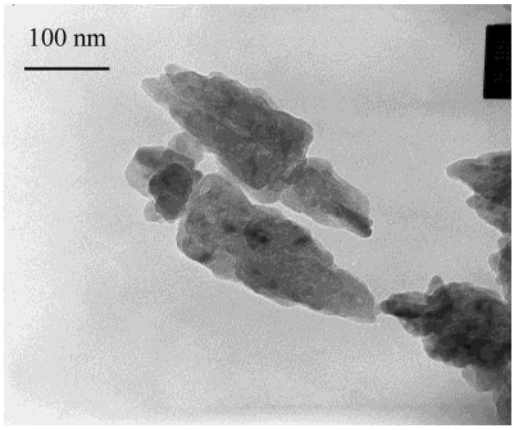

(b)

Figure 7. TEM of ZnO particles obtained at 25 °C and pH 10.5 by precipitation of zinc nitrate with soda in (a) sodium sulfate solution and (b) sodium dodecyl sulfate solution.

This effect did not occur in our configuration. Another important aspect concerns the differences of the role of surfactants on both studies. Whereas Zhong and Matijevic[18] did not detect differences of particle shape as a result of surfactant addition, but rather an increased porosity, our work showed that these additives had an important function in hampering particle aggregation into more complex morphologies (ellipsoids and starlike), as well as isolating some primary particles (nanocrystallites).

Formation Mechanism of Different Morphologies. The transversal crack observed for the ellipsoids precipitated in distilled water at 25 °C and pH 9.5 might be explained by the additive results. As previously proposed, these ellipsoids were formed from a half-ellipsoid followed by the germination of a second half

Table 3. Summary of Experimental Conditions and Results of the Precipitation Tests with Zinc Sulfate and Sodium Hydroxide

test no.	pH	*T* (°C)	particle morphology and size	crystal size (nm)
9	10.5	25	half-ellipsoidal: 350 nm ellipsoidal: 800 nm fibers: 40 nm-diameter small particles: 30 nm	21 × 32
10	10.5	60	small particles:20−30 nm half-ellipsoidal: 100 nm	23 × 33

at its base . At pH 9.5 the two branches grew, keeping the transversal crack in the middle, with formation of one or two branches perpendicularly from this crack occurring only rarely, whereas at pH 10.5, further germination was easier in the crack formed by two branches, allowing the growth of 4 or more perpendicular branches. The origin of the longitudinal crack was more difficult to evaluate because its occurrence was quite rare. The crucial role of pH in the mechanism of branch formation must be further investigated.

Precipitation with Zinc Sulfate and Sodium Hydroxide at pH 10.5. The precipitation using zinc sulfate was aimed at comparing the role of sulfate ion added as zinc salt and as an additive on particle morphology and size.

Table 3 concisely describes experimental conditions and results obtained for the precipitation from zinc sulfate solution with sodium hydroxide in distilled water at pH 10.5. Zinc oxide was produced directly from the studied system. Scherrer's formula led to 21−23-nm crystallite size for (100) and (101) directions and 32−33-nm for (002) direction, indicating again a preferential *c*-axis growth.

At 25 °C, the powder precipitated from the zinc sulfate solution was heterogeneous, presenting some traditional morphologies such as half-ellipsoids (350 nm) and ellipsoids (800 nm), both consisting of 30-nm crystallites grouped in a preferential orientation, as well as 40-nm-diameter fibers of various lengths. Some rare sheets were also detected, probably untransformed zinc hydroxide. Hence, the system is far more heterogeneous than that observed with zinc nitrate in distilled water and zinc nitrate in sodium sulfate solution; nevertheless, it produced intermediate morphologies between separate building blocks and ellipsoids, confirming conclusions drawn from our more homogeneous systems.

A drastic modification of particle morphology was also obtained at 60 °C with zinc sulfate. Small particles from 20 to 60 nm were the main constituents of the precipitated powder. More rarely, some 100-nm half-ellipsoids could be found. The temperature effect on the zinc sulfate system was more intense than that verified on the zinc nitrate system. As a conclusion, a temperature increase up to 60 °C, whatever the system, had a tendency to form bigger crystallites and to strongly limit oriented aggregation.

Conclusions

The direct synthesis of zinc oxide particles with controlled size and morphology was possible using a double-jet precipitation method at room temperature. In addition, the use of an amine base was avoided.

Particles were always constituted by an aggregation of elongated ZnO nanocrystallites, with an aspect ratio of 1.5. The elongation and the well-known polarity effects along the *c*-axis could explain the formation of aggregated structures such as stars with 6 (or more) branches at pH 10.5 and ellipsoids at pH 9.5.

Salt nature produced significant variations on ZnO particles morphology and size. In distilled water at 25 °C, homogeneous 1-μm well-shaped starlike particles were produced with zinc nitrate, whereas a heterogeneous product composed of relatively smaller ellipsoids, half-ellipsoids, and fibers was obtained with zinc sulfate.

The presence of additives allowed synthesis of smaller particles and a considerable change in shape with many ill-shaped particles from half to full ellipsoids. Probably additives adsorbed on crystallites limited nanocrystallite aggregation into bigger particles. These particles could be seen as the embryos of micrometer starlike particles. Because the formation of starlike particles was too sudden to be followed by a kinetics study, the use of growth-inhibiting agents allowed a description of the star birth and growth through the stages (1) formation of a half-ellipsoid with a few nanocrystals, (2) germination of the second half, (3) growth of an ellipsoid, and (4) germination and growth of star branches from the separation between the two halves.

More generally, this study showed the importance of nucleation of nanometric primary particles followed by oriented aggregation to produce uniform submicrometric particles.

Acknowledgment. Dr. Oliveira greatly acknowledges CAPES (Brazil) for providing financial support to her during this work.

CM0213725